

Doppler-Aided Positioning for Fused LEO Navigation Systems

Weiwei Wang , Zhangjian Lu, Ye Tian, Lang Bian, Guoyong Wang and Lixin Zhang

China Academy of Space Technology (Xi'an), Xi'an 710100, China; luzhangjian_504@163.com (Z.L.); tianye_504@163.com (Y.T.); bianl35@163.com (L.B.); wangguoyong321@163.com (G.W.); m13991927780@163.com (L.Z.)

* Correspondence: wangweiwei_504@163.com; Tel.: +86-155-9689-3690

Abstract: Fused LEO navigation systems have been proposed as a low-cost means of supplementing and backing up global navigation satellite system (GNSS) navigation services based on low-earth orbit (LEO) constellations, which means broadcasting navigation signals based on the spectrum and hardware of the currently planned communication constellation. In this paper, we introduce Doppler-aided positioning to fused LEO navigation systems, which can improve the positioning performance and availability of fused LEO navigation systems by addressing insufficient pseudorange measures caused by insufficient navigation resources or the early stages of system construction. Theoretical analysis and simulation results show that Doppler-aided positioning based on the weighted least squares (WLS) method can improve the positioning accuracy of pseudorange positioning and achieve 95% three-dimensional errors within 21 m, even if the number of pseudorange measurements is less than four. Therefore, Doppler-aided positioning can expand the application scenarios of independent navigation services for fused LEO navigation systems.

Keywords: Doppler-aided positioning; fused LEO navigation systems; weighted least squares method; Cramér–Rao lower bound



Citation: Wang, W.; Lu, Z.; Tian, Y.; Bian, L.; Wang, G.; Zhang, L. Doppler-Aided Positioning for Fused LEO Navigation Systems. *Aerospace* **2023**, *10*, 864. <https://doi.org/10.3390/aerospace10100864>

Academic Editor: Kamil Krasuski

Received: 31 August 2023

Revised: 27 September 2023

Accepted: 28 September 2023

Published: 1 October 2023



Copyright: © 2023 by the authors. Licensee MDPI, Basel, Switzerland. This article is an open access article distributed under the terms and conditions of the Creative Commons Attribution (CC BY) license (<https://creativecommons.org/licenses/by/4.0/>).

1. Introduction

In recent years, LEO constellation construction, such as StarLink, OneWeb, and GW, has entered a booming stage, with hundreds or thousands of satellites included in these constellations [1]. These LEO satellites have distinct advantages over medium- to high-earth orbit satellites, including high signal strength, fast geometric changes, and a large Doppler frequency shift, which means that they can complement traditional GNSS constellations, and have significant advantages in enhancing accuracy, integrity, continuity, and the availability of navigation service [2,3]. Therefore, LEO satellites enhancing navigation services have become a hot topic in the current field of satellite navigation.

The existing applications of LEO satellites to enhance navigation services mainly focus on enhancing GNSS and independently providing positioning, navigation, and timing (PNT) services. In terms of GNSS enhancement, the research content focuses on improving the orbit determination accuracy of GNSS satellites using LEO satellites [4], and achieving fast convergence of precise point positioning (PPP) through navigation signals broadcast by LEO satellites [5].

There are two main methods to offer independent PNT services using LEO satellites. One is to design new navigation signals and payloads to support navigation capabilities. For example, Satelles company [6] designed a satellite time and location (STL) signal to provide PNT services. Reid et al. [7] studied an LEO navigation system using independent payloads, which has a higher cost. The other method is to utilize existing communication satellite payloads to achieve LEO navigation enhancement, which is also called a fused LEO navigation system. Because the operating frequency of communication satellites is usually distributed in the Ku-Ka band, utilizing the frequency band and hardware of existing communication payloads can avoid interference and deception against L-band navigation

signals, effectively compensate for the service loss caused by L-band navigation signal failure [8], and achieve the supplementation and backup of GNSS positioning services. At present, studies on providing navigation services based on existing communication satellite payloads focus on the opportunity navigation framework, which utilizes Doppler measurements to determine receiver position and velocity [9–11].

To solve the problem of low positioning accuracy in Doppler measurements, an increasing number of studies have discussed the use of code pseudorange or carrier phase in navigation services based on communication satellites. For example, Khalife et al. [12] designed a hosted receiver to obtain carrier phase values, and obtained a horizontal positioning result of 7.7 m. The University of Texas [13,14] proposed the fused LEO GNSS system without any sacrifice in performance, and eliminated the cost of hosted hardware on board. These above methods are based on the analysis of large LEO constellations, such as Starlink. However, LEO communication constellations can provide fewer pseudorange measurements in circumstances where navigation resources are insufficient or in the early stages of system construction, making it impossible to meet the requirements of positioning; that is, there are fewer than four pseudorange measurements at the same time.

In order to address the above problems, we propose a method of applying Doppler-aided positioning to fused LEO navigation systems, where some satellites broadcast navigation signals to provide pseudorange and Doppler measurements, while other visible satellites with other functions provide Doppler measurements. Based on the pseudorange and Doppler measurements mentioned above, user positioning is achieved by Doppler-aided positioning. This method can improve the positioning performance and availability of high-security positioning in fused LEO navigation systems and expand the application range of LEO navigation services.

In this paper, the principle of the Doppler-aided positioning method in fused LEO navigation systems is first introduced, and then the positioning performance of Doppler-aided positioning based on WLS is analyzed. Finally, we provide discussion and conclusions.

2. Doppler-Aided Positioning for Fused LEO Navigation Systems

Doppler-aided positioning can be divided into two types. One is where Doppler measurements are not directly involved in positioning and are commonly used to assist in smoothing pseudorange or shortening initial positioning time [15,16]. The other involves Doppler measurements directly in the navigation positioning process by combining them with pseudorange measurements to achieve user positioning. In 2011, Li et al. [17] provided position services based on Doppler and pseudorange measurements of GNSS, and the results showed that the Doppler-aided method based on the WLS method could improve positioning performance. In 2020, Vincent et al. [18] theoretically analyzed GNSS pseudorange positioning and the WLS method based on pseudorange and Doppler measurements. The results showed that Doppler information can improve positioning accuracy in urban canyons or indoor environments. In 2022, Jiang et al. [19] proposed a cooperative positioning method that utilizes LEO satellite Doppler measurements, GNSS pseudorange, and GNSS Doppler measurements. The positioning accuracy can reach about 250 m. So far, Doppler-aided positioning has not been applied to independent navigation services for LEO constellations.

In this paper, we propose a method of applying Doppler-aided positioning to fused LEO navigation systems, enabling independent navigation positioning services. Users receive signals from multiple satellites, with some satellites transmitting ranging bursts that generate both pseudorange and Doppler measurements. Other visible satellites transmit bursts for other functions, which can generate Doppler measurements without known signal structures, as shown in Figure 1. User positioning is achieved based on the aforementioned pseudorange and Doppler measurements. This method can achieve high-security navigation positioning services for fused LEO navigation systems, balance communication, internet, or other missions, and serve as a supplementary and backup to GNSS positioning services.

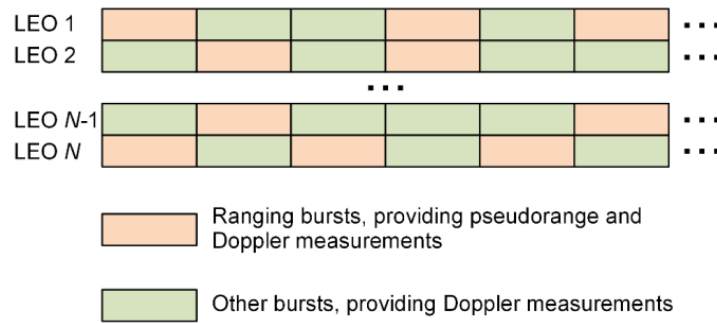


Figure 1. LEO satellites broadcast bursts in fused LEO navigation systems. Orange rectangles represent ranging bursts, which can provide both pseudorange and Doppler measurements, while green rectangles represent other bursts, which can provide Doppler measurements.

It is worth mentioning that in this method, LEO satellites need to be equipped with GNSS receivers to receive signals from medium- to high-earth-orbit GNSS satellites for precise orbit and clock offset determination, as shown in Figure 2. LEO satellites can be equipped with an oven-controlled crystal oscillator (OCXO) to save costs and improve clock offset accuracy through rapid measurement and rapid ephemeris updates.

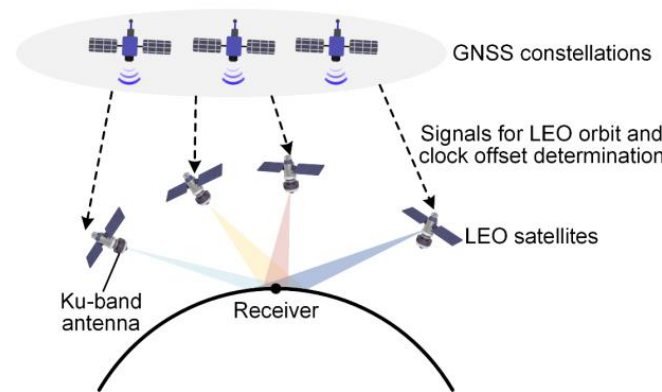


Figure 2. Fused LEO navigation system.

2.1. Principle of Doppler-Aided Positioning

The pseudorange positioning equation can be written as

$$\rho_r^s = \|\mathbf{r}^s - \mathbf{r}_r\| + c(\delta t_r - \delta t^s) + I + T + c \cdot dR^s + dE_r^s + \varepsilon_\rho \tag{1}$$

where ρ_r^s is the pseudorange measurement; $\mathbf{r}^s = [x^s, y^s, z^s]^T$ is the satellite position vector; $\mathbf{r}_r = [x_r, y_r, z_r]^T$ is the receiver position vector; c is the speed of light; δt_r and δt^s are the clock offsets between the receiver and the satellite, respectively; I is the ionospheric delay; T is the troposphere delay; ε_ρ is all errors that have not been modeled. dR^s is the delay caused by the relativistic effect of satellite clock offset, which can be expressed as

$$dR^s = -2 \frac{\mathbf{r}^s \cdot \dot{\mathbf{r}}^s}{c^2} \tag{2}$$

where $\dot{\mathbf{r}}^s = [v_x^s, v_y^s, v_z^s]^T$ is the satellite velocity vector and dE_r^s is the delay caused by the Sagnac effect, which can be expressed by

$$dE_r^s = \frac{\omega_e}{c^2} (x^s \cdot y_r - y^s \cdot x_r) \tag{3}$$

where ω_e is the angular speed of the earth’s rotation.

The Doppler effect is caused by the relative motion between the transmitter and receiver, and the Doppler shift can be expressed as

$$D_r^s = f_R - f_T = -\frac{v_{los}}{c} f_T = -\frac{v_{los}}{\lambda_f} \tag{4}$$

where f_R and f_T are, respectively, the receiving and transmitting frequencies of navigation signals, and v_{los} is the relative velocity in the direction of the receiver and satellite connection. If the satellite and receiver move toward each other, the Doppler shift is positive. Otherwise, the Doppler shift is negative. v_{los} is also known as the pseudorange rate, and its expression is:

$$v_{los} = \left(\dot{\mathbf{r}}^s - \dot{\mathbf{r}}_r \right) \cdot \frac{\mathbf{r}^s - \mathbf{r}_r}{\|\mathbf{r}^s - \mathbf{r}_r\|} = \dot{\rho}_r^s \tag{5}$$

where $\dot{\mathbf{r}}_r = [v_{r,x}, v_{r,y}, v_{r,z}]^T$ is the user speed vector; $\dot{\rho}_r^s$ is the pseudorange rate, the unit is m/s, which is the first derivative of the pseudorange concerning time, and the derivation of Equation (4) is

$$\dot{\rho}_r^s = -\lambda_f \cdot D_r^s = \left(\dot{\mathbf{r}}^s - \dot{\mathbf{r}}_r \right) \cdot \frac{\mathbf{r}^s - \mathbf{r}_r}{\|\mathbf{r}^s - \mathbf{r}_r\|} + c \left(\delta \dot{t}_r - \delta \dot{t}^s \right) + \dot{I} + \dot{T} + c \cdot d\dot{R}^s + d\dot{E}_r^s + \varepsilon_D \tag{6}$$

where $\delta \dot{t}_r$ and $\delta \dot{t}^s$ are the clock drifts of satellites and receivers, respectively; \dot{I} and \dot{T} are the change rates of the ionosphere and troposphere delay, respectively; ε_D is all errors that have not been modeled; $d\dot{R}^s$ is a delay caused by the relativistic effect of satellite clock offset, which can be expressed as

$$d\dot{R}^s = -2 \frac{\dot{\mathbf{r}}^s \cdot \dot{\mathbf{r}}^s + \mathbf{r}^s \cdot \ddot{\mathbf{r}}^s}{c^2} \tag{7}$$

where $\ddot{\mathbf{r}}^s$ is the satellite acceleration vector and $d\dot{E}_r^s$ is the delay caused by the Sagnac effect, which can be written as

$$d\dot{E}_r^s = \frac{\omega_e}{c^2} \left(v_x^s \cdot y_r + v_{r,y} \cdot x^s - v_y^s \cdot x_r - v_{r,x} \cdot y^s \right) \tag{8}$$

and in the above equation, the satellite speed, position, and clock offset can be obtained from the ephemeris data.

Assuming that the receiver can receive n pseudorange measurements and m Doppler measurements of an LEO constellation, generally $m \geq n$, the positioning equations can be obtained as

$$\left\{ \begin{array}{l} \rho_r^{s,1} = \|\mathbf{r}^{s,1} - \mathbf{r}_r\| + c(\delta t_r - \delta t^{s,1}) + I + T + c \cdot dR^{s,1} + dE_r^{s,1} + \varepsilon_{\rho,1} \\ \dots \\ \rho_r^{s,n} = \|\mathbf{r}^{s,n} - \mathbf{r}_r\| + c(\delta t_r - \delta t^{s,n}) + I + T + c \cdot dR^{s,n} + dE_r^{s,n} + \varepsilon_{\rho,n} \\ \dot{\rho}_r^{s,1} = -\lambda_f \cdot D_r^{s,1} = \left(\dot{\mathbf{r}}^{s,1} - \dot{\mathbf{r}}_r \right) \cdot \frac{\mathbf{r}^{s,1} - \mathbf{r}_r}{\|\mathbf{r}^{s,1} - \mathbf{r}_r\|} + c \left(\delta \dot{t}_r - \delta \dot{t}^{s,1} \right) + \dot{I} + \dot{T} + c \cdot d\dot{R}^{s,1} + d\dot{E}_r^{s,1} + \varepsilon_{D,1} \\ \dots \\ \dot{\rho}_r^{s,m} = -\lambda_f \cdot D_r^{s,m} = \left(\dot{\mathbf{r}}^{s,m} - \dot{\mathbf{r}}_r \right) \cdot \frac{\mathbf{r}^{s,m} - \mathbf{r}_r}{\|\mathbf{r}^{s,m} - \mathbf{r}_r\|} + c \left(\delta \dot{t}_r - \delta \dot{t}^{s,m} \right) + \dot{I} + \dot{T} + c \cdot d\dot{R}^{s,m} + d\dot{E}_r^{s,m} + \varepsilon_{D,m} \end{array} \right. \tag{9}$$

and by solving the above equations, user positioning can be achieved.

The state vector \mathbf{X} based on pseudorange and Doppler measurements is an eight-dimensional vector, which is

$$\begin{aligned} \mathbf{X} &= \left[\mathbf{r}_r \ \dot{\mathbf{r}}_r \ c\delta t_r \ c\delta \dot{t}_r \right] \\ &= \left[x_r \ y_r \ z_r \ v_{x,r} \ v_{y,r} \ v_{z,r} \ c\delta t_r \ c\delta \dot{t}_r \right] \in \mathbf{R}^8 \end{aligned} \tag{10}$$

including the receiver position vector, velocity vector, clock offset, and clock drift.

2.2. Weighted Least Squares Method

Considering that different types of measurements have different measurement errors, we chose the WLS method to solve the user position, which is commonly used for Doppler-aided positioning for GNSS. This method has two advantages. On the one hand, the WLS method can better adapt to different types of measurement data and improve the robustness of positioning by using weighted techniques to handle noise. On the other hand, the WLS method can improve positioning accuracy compared to the least-squares method [17].

WLS requires several iterations to solve multivariate nonlinear equations. At the position of the k -th iteration, the positioning Equation (9) is linearized, and can be written

$$G\Delta X = G \begin{bmatrix} \Delta x_r \\ \Delta y_r \\ \Delta z_r \\ \Delta v_{x,r} \\ \Delta v_{y,r} \\ \Delta v_{z,r} \\ \Delta c\delta t_r \\ \Delta c\dot{\delta}t_r \end{bmatrix} = \begin{bmatrix} \rho_r^{s,1} - \rho_r^{s,1}(X_k) \\ \dots \\ \rho_r^{s,n} - \rho_r^{s,n}(X_k) \\ \dot{\rho}_r^{s,1} - \dot{\rho}_r^{s,1}(X_k) \\ \dots \\ \dot{\rho}_r^{s,m} - \dot{\rho}_r^{s,m}(X_k) \end{bmatrix} = \mathbf{b} \tag{11}$$

where G is a geometric matrix, its expression is

$$G = \begin{bmatrix} \frac{\partial \rho_r^{s,1}}{\partial r_r} & \frac{\partial \rho_r^{s,1}}{\partial \dot{r}_r} & \frac{\partial \rho_r^{s,1}}{\partial \delta t_r} & \frac{\partial \rho_r^{s,1}}{\partial \dot{\delta}t_r} \\ \dots \\ \frac{\partial \rho_r^{s,n}}{\partial r_r} & \frac{\partial \rho_r^{s,n}}{\partial \dot{r}_r} & \frac{\partial \rho_r^{s,n}}{\partial \delta t_r} & \frac{\partial \rho_r^{s,n}}{\partial \dot{\delta}t_r} \\ \frac{\partial \dot{\rho}_r^{s,1}}{\partial r_r} & \frac{\partial \dot{\rho}_r^{s,1}}{\partial \dot{r}_r} & \frac{\partial \dot{\rho}_r^{s,1}}{\partial \delta t_r} & \frac{\partial \dot{\rho}_r^{s,1}}{\partial \dot{\delta}t_r} \\ \dots \\ \frac{\partial \dot{\rho}_r^{s,m}}{\partial r_r} & \frac{\partial \dot{\rho}_r^{s,m}}{\partial \dot{r}_r} & \frac{\partial \dot{\rho}_r^{s,m}}{\partial \delta t_r} & \frac{\partial \dot{\rho}_r^{s,m}}{\partial \dot{\delta}t_r} \end{bmatrix} = \begin{bmatrix} \frac{\partial \rho_r^{s,1}}{\partial r_r} & \mathbf{0}_{1 \times 3} & 1 & 0 \\ \dots \\ \frac{\partial \rho_r^{s,n}}{\partial r_r} & \mathbf{0}_{1 \times 3} & 1 & 0 \\ \frac{\partial \dot{\rho}_r^{s,1}}{\partial r_r} & \frac{\partial \dot{\rho}_r^{s,1}}{\partial \dot{r}_r} & 0 & 1 \\ \dots \\ \frac{\partial \dot{\rho}_r^{s,m}}{\partial r_r} & \frac{\partial \dot{\rho}_r^{s,m}}{\partial \dot{r}_r} & 0 & 1 \end{bmatrix}_{(n+m) \times 8} \tag{12}$$

and

$$\frac{\partial \rho_r^s}{\partial r_r} = \frac{(\mathbf{r}^s - \mathbf{r}_r)^T (\dot{\mathbf{r}}^s - \dot{\mathbf{r}}_r) (\mathbf{r}^s - \mathbf{r}_r)^T}{\|\mathbf{r}^s - \mathbf{r}_r\|^3} - \frac{(\dot{\mathbf{r}}^s - \dot{\mathbf{r}}_r)^T}{\|\mathbf{r}^s - \mathbf{r}_r\|} \tag{13}$$

$$\frac{\partial \dot{\rho}_r^s}{\partial \dot{r}_r} = -\frac{(\mathbf{r}^s - \mathbf{r}_r)^T}{\|\mathbf{r}^s - \mathbf{r}_r\|} \tag{14}$$

and we apply the WLS method to Doppler-aided positioning for real-time positioning. That is, set a weight w_ρ or $w_{\dot{\rho}}$ for each measurement, and the larger the weight, the greater its role in the solution of the WLS method. In this paper, the weight value is set to the reciprocal of the standard deviation of measurement error, which can be written as

$$\begin{aligned} w_\rho &= \frac{1}{\sigma_\rho} \\ w_{\dot{\rho}} &= \frac{1}{\sigma_{\dot{\rho}}} \end{aligned} \tag{15}$$

and according to the above equation, the WLS method is used to estimate, that is, minimize the sum of residual squares, which is

$$\begin{aligned} \Delta X &= \operatorname{argmin}[G\Delta X - \mathbf{b}]^T W[G\Delta X - \mathbf{b}] \\ &= (\mathbf{G}^T W \mathbf{G})^{-1} \mathbf{G}^T W \mathbf{b} \end{aligned} \tag{16}$$

When the WLS method is used to obtain user position and the measurement error vector ε in Equation (9) is retained, the matrix positioning Equation (11) can be rewritten as

$$\begin{aligned} G(\Delta X + \varepsilon_X) &= \mathbf{b} + \varepsilon \\ \Delta X + \varepsilon_X &= \left(G^T W G\right)^{-1} G^T W (\mathbf{b} + \varepsilon) \\ \varepsilon_X &= \left(G^T W G\right)^{-1} G^T W \varepsilon \end{aligned} \quad (30)$$

and the above equation indicates the relationship between measurement error and positioning error. According to the definition of the CRLB, the positioning error can be obtained as

$$\begin{aligned} \text{Var}(\varepsilon_X) &\approx \text{Var}\left[\left(G^T W G\right)^{-1} G^T W \varepsilon\right] \\ &\geq \left[\left(G^H W G\right)^{-1} G^H W\right] I^{-1}(\varepsilon) \left[\left(G^H W G\right)^{-1} G^H W\right]^T \end{aligned} \quad (31)$$

and during the positioning process, by incorporating matrixes (G , W , and $I(\varepsilon)$) into the above equation, the CRLB of Doppler-aided positioning based on the WLS method can be obtained.

4. Doppler-Aided Positioning Simulation Results

In this section, we first introduce the simulation parameters. Then, we simulate Doppler-aided positioning based on the WLS method and analyze its CRLB and positioning results.

4.1. Simulation Parameters

In the LEO constellation simulation, we adopt a hybrid configuration of near-polar orbit and Walker constellations to achieve global coverage. A mega-LEO constellation consisting of 390 satellites was simulated, including 120 satellites in inclined orbit and 270 satellites in near-polar orbit. The constellation parameters are shown in Table 1, and the three-dimensional diagram is shown in Figure 3. The average number of visible satellites in this constellation is greater than 10, which meets pseudorange positioning requirements when the constellation provides independent navigation services, as shown in Figure 4.

References [11,21] indicate that the measurement accuracy of Doppler frequency can be better than 1 Hz, so in this section, we set the Doppler measurement accuracy to 1 Hz. The simulation position is set at BJT1, and the signal frequency is referred to as in reference [13]. Reference [13] analyzed the ranging error, satellite orbit, and clock error of the LEO signal. Based on the analysis of reference [13], we set simulation parameters, as shown in Table 2.

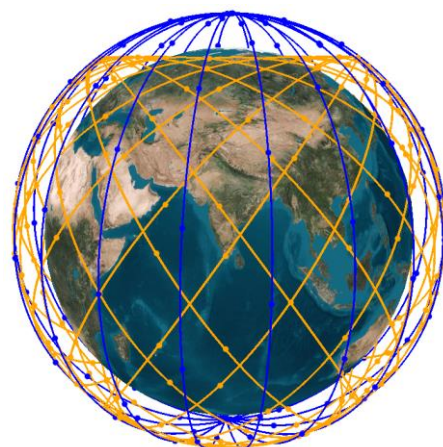
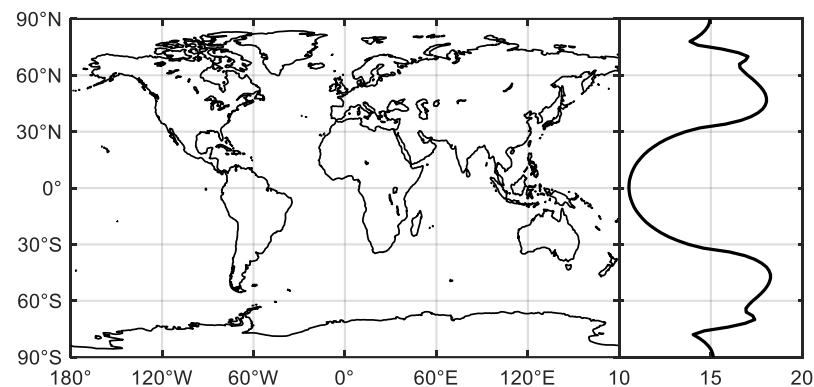


Figure 3. Simulated LEO constellation. Blue points represent near-polar orbit satellites, and orange points represent satellites in the Walker constellation.

Table 1. Simulation parameters of the LEO constellation.

Parameters	LEO Constellation	
Configuration	Near-polar orbit	Walker
Number of satellites	120	270
Number of orbital planes	10	18
Number of satellites per orbital plane	12	15
Orbital height	1050 km	1000 km
Orbital inclination	89°	55°
Eccentricity	0	0

**Figure 4.** Distribution of average visible satellites with latitude. The simulation duration is 24 h, and the user elevation threshold is 10°.**Table 2.** Simulation parameters.

Simulation Parameters	Value
Position	BJF1: 39.61° N, 115.89° E, 87.47 m
Frequency	12 GHz
User ranging error	0.105 m
RMS error of satellite orbit	R: 0.059 m, A: 0.093 m, C: 0.083 m
Satellite clock offset RMS error	0.022 m
Frequency measurement accuracy	1 Hz

4.2. Simulated Positioning Results

In this section, the WLS method is employed for Doppler-aided positioning to achieve real-time positioning. The duration of positioning is 2 h, with one real-time positioning result output per second, resulting in a total of 7200 positioning results. As shown in Figure 5, the average number of visible satellites during the simulation period was 17.52, which corresponds to an average Doppler measurement number of 17.52. The number of pseudorange measurements remains constant in each simulation, with satellites randomly selected from the visible satellites to provide the pseudorange measurements.

As shown in Figure 6, when eight satellites provide pseudorange measurements, the theoretical three-dimensional positioning error (σ_{3D}) for pseudorange positioning and the CRLB for Doppler-aided positioning have little difference. By using the weighted least squares method, the 95% three-dimensional positioning errors for pseudorange positioning and Doppler-aided positioning were 1.23 m and 0.72 m, respectively, with an improvement of 41.46%, which is related to the weighting matrix W in the WLS method.

As shown in Figure 7, when four satellites provide pseudorange measurements, the theoretical three-dimensional positioning error (σ_{3D}) for pseudorange positioning is 15.32 m, and the CRLB for Doppler-aided positioning is 4.59 m. The 95% three-dimensional positioning errors of pseudorange positioning and Doppler-aided positioning are 24.43 m and 4.97 m, respectively. This indicates that the geometric structure of the four satellites

is poor, and that the positioning error is large during pseudorange positioning. Doppler information can improve geometric structure, thereby improving positioning accuracy.

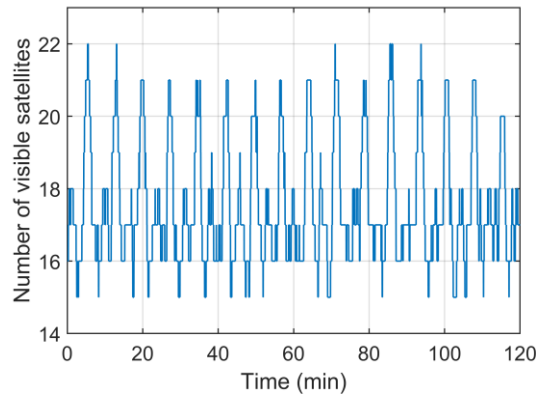


Figure 5. Number of visible satellites during the simulation period.

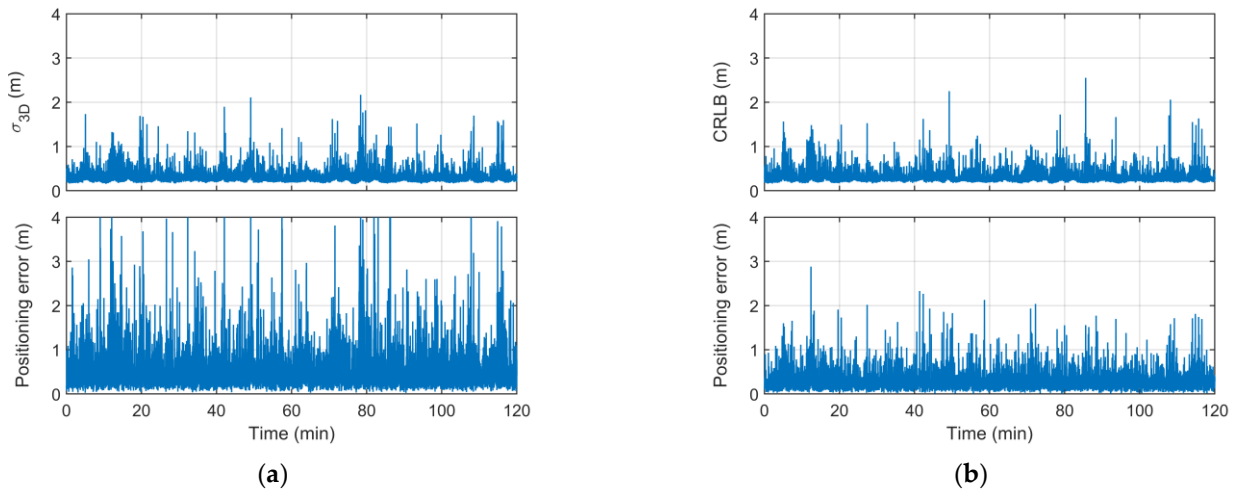


Figure 6. Simulation results of pseudorange positioning and Doppler-aided positioning. Eight random satellites provide pseudorange measurements. (a) Pseudorange positioning results; (b) Doppler-aided positioning results.

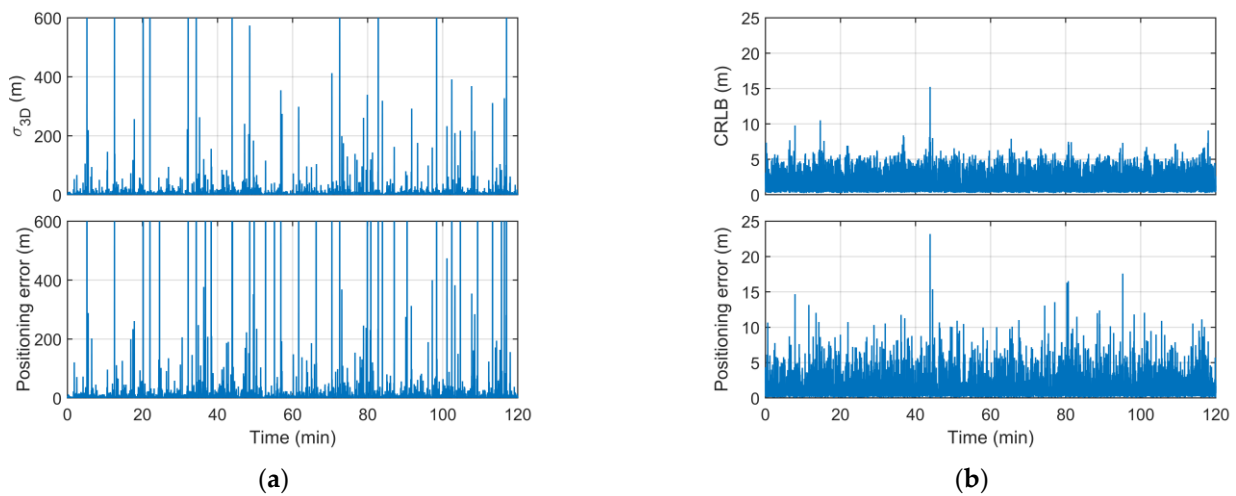


Figure 7. Simulation results of pseudorange positioning and Doppler-aided positioning. Four random satellites provide pseudorange measurements. (a) Pseudorange positioning results; (b) Doppler-aided positioning results.

As shown in Figure 8, when the number of satellites providing pseudorange measurements is three, two, one, and zero, the 95% three-dimensional positioning errors are 10.46 m, 14.00 m, 20.37 m, and 19.95 m, respectively. The results show that when the number of pseudorange measurements is less than four, pseudorange positioning cannot achieve positioning, while other Doppler measurements provided by Doppler-aided positioning can assist in real-time positioning, with a 95% three-dimensional error maintained within 21 m, which can expand the application field of high-security positioning in fused LEO navigation systems.

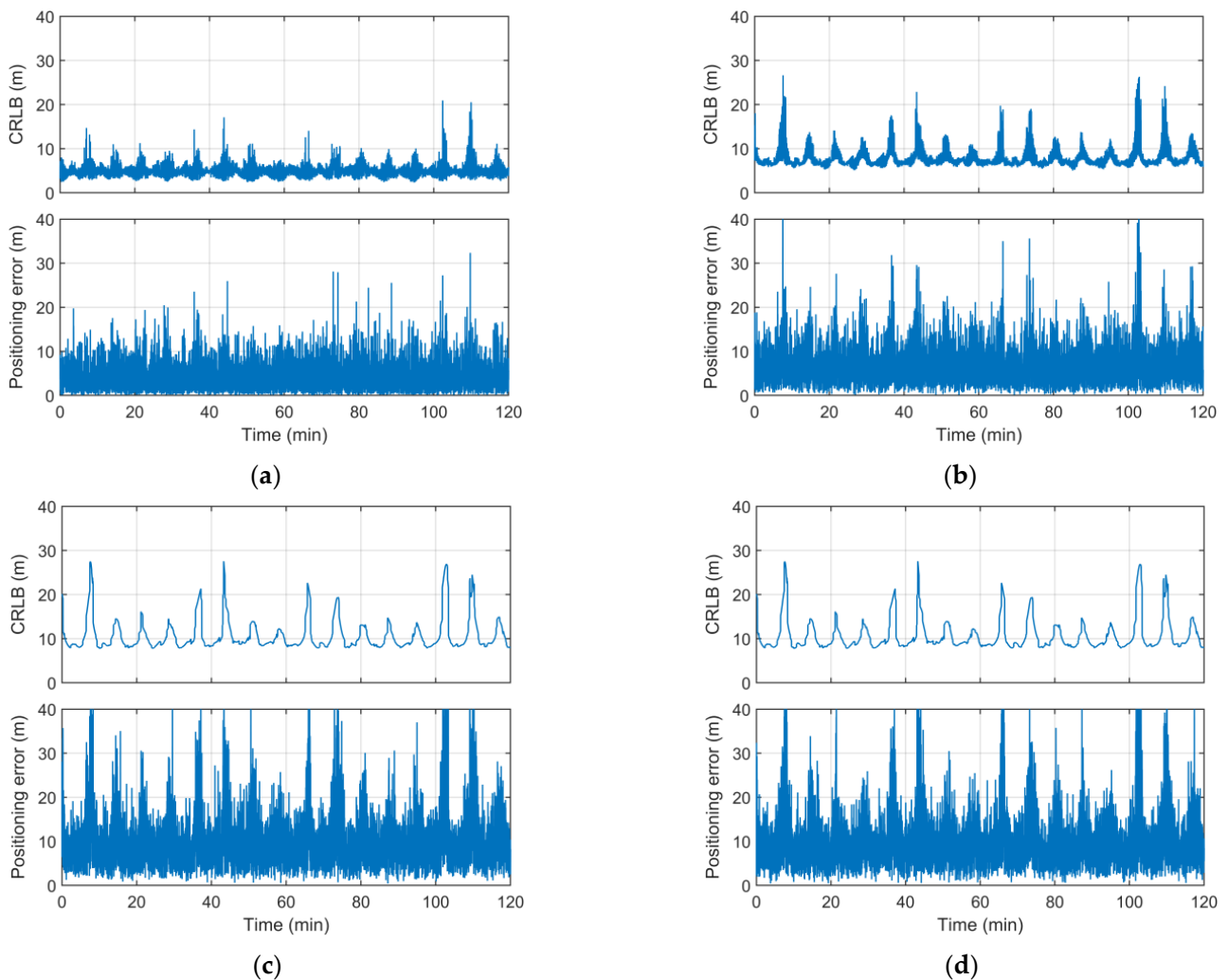


Figure 8. Theoretical and simulation results of Doppler-aided positioning. (a) Three satellites provide pseudorange measurements; (b) two satellites provide pseudorange measurements; (c) one satellite provides pseudorange measurements; (d) no satellites provide pseudorange measurements.

From Figure 9 and Table 3, it can be seen that when the number of pseudorange measurements approaches four, the positioning error increases sharply. With the reduction of pseudorange measurements, the improvement effect of pseudorange measurements is increasing. Doppler-aided positioning can still be achieved when the pseudorange measurements are less than four. In summary, pseudorange measurements can improve positioning accuracy and expand the application range of pseudorange positioning.

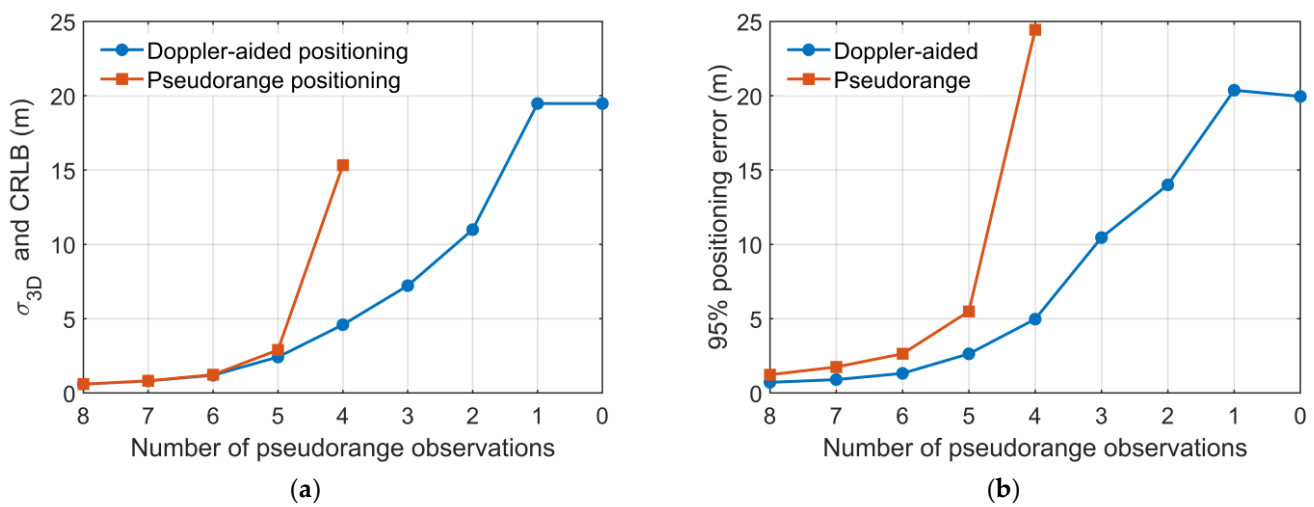


Figure 9. Relationship between 95% positioning error with the number of pseudorange measurements: (a) 95% theoretical positioning error; (b) 95% simulation positioning error.

Table 3. The 95% three-dimensional error of Doppler-aided positioning.

Number of Pseudorange Measurements	Doppler-Aided Positioning	Pseudorange Positioning	Increase Amplitude
8	0.72 m	1.23 m	41.46%
7	0.90 m	1.75 m	48.57%
6	1.32 m	2.64 m	49.98%
5	2.64 m	5.49 m	51.91%
4	4.97 m	24.43 m	79.66%
3	10.46 m	-	-
2	14.00 m	-	-
1	20.37 m	-	-
0	19.95 m	-	-

5. Discussion

Doppler-aided positioning is frequently applied in GNSS and has no significant improvement compared to traditional pseudorange positioning when there is a large number of visible GNSS satellites. Therefore, Doppler-aided positioning is typically used to improve positioning accuracy in urban canyons or indoor environments [17,18].

In fused LEO navigation systems, LEO constellations are usually not built for navigation services and need to balance other tasks. When navigation resources are insufficient, it can result in a few pseudorange measurements being received at the same time. Moreover, LEO satellites typically have characteristics such as a small coverage area and narrow beam width, which can lead to a few pseudorange measurements being received at the same time during the early stages of system construction. In these situations, due to insufficient measurements, traditional pseudorange positioning may not be applicable, or have low accuracy. Therefore, Doppler-aided positioning can be applied to the above situations, improving the accuracy and availability of independent positioning and expanding the application scenarios of fused LEO navigation systems.

In this paper, we study Doppler-aided positioning for fused LEO navigation systems using the WLS method. The WLS method only utilizes Doppler and pseudorange measurements at the current time and can achieve real-time positioning. When there are few visible satellites, Doppler measurements can provide more information. Therefore, compared to pseudorange positioning, Doppler-aided positioning can significantly improve positioning accuracy.

6. Conclusions

In the development process of fused LEO navigation systems, when in the early stages of system construction or when navigation resources are insufficient, it can lead to the problem of insufficient pseudorange measurements. In these situations, due to insufficient measurements, traditional pseudorange positioning may not be applicable, or have low accuracy. Therefore, it is necessary to study a more suitable positioning method for fused LEO navigation systems.

In order to address the above problems, this paper proposes a method of applying Doppler-aided positioning to fused LEO navigation systems, enabling independent navigation positioning services. Users receive signals from multiple satellites, some of which transmit ranging bursts that generate both pseudorange and Doppler measurements. Other visible satellites transmit bursts for various tasks, which can generate Doppler measurements without known signal structures. Based on the pseudorange and Doppler measurements mentioned above, user positioning is achieved.

Theoretical and simulation results show that Doppler-aided positioning based on the WLS method can improve pseudorange positioning accuracy and can still achieve positioning even when the pseudorange measurement is less than four, and the 95% three-dimensional positioning error using the WLS method is maintained within 21 m. When there are few visible satellites, Doppler-aided positioning improves positioning accuracy more significantly.

This method balances communication, internet, or other missions, improves the positioning performance and availability of high-security positioning in fused LEO navigation systems, and expands the application range of fused LEO navigation systems.

Author Contributions: Conceptualization, W.W., Z.L. and L.B.; methodology, W.W.; validation, W.W., Z.L. and Y.T.; resources, L.B., Y.T., G.W. and L.Z.; writing—original draft preparation, W.W. and Z.L.; writing—review and editing, Z.L., Y.T., L.B., G.W. and L.Z.; funding acquisition, L.B., G.W. and L.Z. All authors have read and agreed to the published version of the manuscript.

Funding: This work was supported in part by the National Natural Science Foundation of China under Grant 12373079, the Key Research Program under Grant 2019-JCJQ-ZD-342-00, and the Pro-research Project for Equipment of General Information System under Grant 315067105.

Data Availability Statement: Not applicable.

Conflicts of Interest: The authors declare no conflict of interest.

References

1. Ruan, Y.; Hu, M.; Yun, C. Advances and prospects of the configuration design and control research of the LEO mega-constellations. *Chin. Space Sci. Technol.* **2022**, *42*, 1–15.
2. Ge, H.; Li, B.; Jia, S.; Nie, L.; Wu, T.; Yang, Z.; Shang, J.; Zheng, Y.; Ge, M. LEO Enhanced Global Navigation Satellite System (LeGNSS): Progress, opportunities, and challenges. *Geo Spat. Inf. Sci.* **2022**, *25*, 1–13. [[CrossRef](#)]
3. Prol, F.S.; Ferre, R.M.; Saleem, Z.; Välisuo, P.; Pinell, C.; Lohan, E.S.; Elsanhoury, M.; Elmusrati, M.; Islam, S.; Celikbilek, K.; et al. Position, navigation, and timing (PNT) through low earth orbit (LEO) satellites: A survey on current status, challenges, and opportunities. *IEEE Access* **2022**, *10*, 83971–84002. [[CrossRef](#)]
4. Li, B.; Ge, H.; Ge, M.; Nie, L.; Shen, Y.; Schuh, H. LEO enhanced Global Navigation Satellite System (LeGNSS) for real-time precise positioning services. *Adv. Space Res.* **2019**, *63*, 73–93. [[CrossRef](#)]
5. Li, X.; Ma, F.; Li, X.; Lv, H.; Bian, L.; Jiang, Z.; Zhang, X. LEO constellation-augmented multi-GNSS for rapid PPP convergence. *J. Geod.* **2019**, *93*, 749–764. [[CrossRef](#)]
6. Lawrence, D.; Cobb, H.S.; Gutt, G.; Tremblay, F.; Laplante, P.; O'Connor, M. Test Results from a LEO-Satellite-Based Assured Time and Location Solution. In Proceedings of the 2016 International Technical Meeting of the Institute of Navigation, Monterey, CA, USA, 25–28 January 2016.
7. Reid, T.G.; Neish, A.M.; Walter, T.F.; Enge, P.K. Leveraging commercial broadband LEO constellations for navigating. In Proceedings of the 29th International Technical Meeting of the Satellite Division of The Institute of Navigation (ION GNSS+ 2016), Portland, OR, USA, 12–16 September 2016.
8. Xiao, Y.; Li, L.; Chang, J.; Yu, J.; Gong, W.; Liang, G. Navigation Method for Terrestrial Users Based on Beidou Ka Inter Satellite Links. *Chin. J. Aeronaut.* **2019**, *40*, 320.

9. Khalife, J.; Neinavaie, M.; Kassas, Z.M. Blind Doppler tracking from OFDM signals transmitted by broadband LEO satellites. In Proceedings of the 2021 IEEE 93rd Vehicular Technology Conference (VTC2021-Spring), Helsinki, Finland, 25–28 April 2021.
10. Orabi, M.; Khalife, J.; Kassas, Z.M. Opportunistic navigation with Doppler measurements from Iridium Next and Orbcomm LEO satellites. In Proceedings of the 2021 IEEE Aerospace Conference (50100), Big Sky, MT, USA, 6–13 March 2021.
11. Neinavaie, M.; Khalife, J.; Kassas, Z.M. Acquisition, Doppler tracking, and positioning with Starlink LEO satellites: First results. *IEEE Trans. Aerosp. Electron. Syst.* **2021**, *58*, 2606–2610. [[CrossRef](#)]
12. Khalife, J.; Neinavaie, M.; Kassas, Z.M. The first carrier phase tracking and positioning results with Starlink LEO satellite signals. *IEEE Trans. Aerosp. Electron. Syst.* **2021**, *58*, 1487–1491. [[CrossRef](#)]
13. Iannucci, P.A.; Humphreys, T.E. Economical fused LEO GNSS. In Proceedings of the 2020 IEEE/ION Position, Location and Navigation Symposium (PLANS), Portland, OR, USA, 20–23 April 2020.
14. Iannucci, P.A.; Humphreys, T.E. Fused low-Earth-orbit GNSS. In *IEEE Transactions on Aerospace and Electronic Systems*; IEEE: Piscataway, NJ, USA, 2022; p. 1.
15. Bahrami, M. Getting back on the sidewalk: Doppler-aided autonomous positioning with single-frequency mass market receivers in urban areas. In Proceedings of the 22nd International Technical Meeting of The Satellite Division of the Institute of Navigation (ION GNSS 2009), Savannah, GA, USA, 22–25 September 2009.
16. Chen, H.W.; Wang, H.S.; Chiang, Y.T.; Chang, F.R. A new coarse-time GPS positioning algorithm using combined Doppler and code-phase measurements. *GPS Solut.* **2014**, *18*, 541–551. [[CrossRef](#)]
17. Li, L.; Zhong, J.; Zhao, M. Doppler-aided GNSS position estimation with weighted least squares. *IEEE Trans. Veh. Technol.* **2011**, *60*, 3615–3624. [[CrossRef](#)]
18. Vincent, F.; Vilà-Valls, J.; Besson, O.; Medina, D.; Chaumette, E. Doppler-aided positioning in GNSS receivers-A performance analysis. *Signal Process.* **2020**, *176*, 107713. [[CrossRef](#)]
19. Jiang, M.; Qin, H.; Zhao, C.; Sun, G. LEO Doppler-aided GNSS position estimation. *GPS Solut.* **2022**, *26*, 31. [[CrossRef](#)]
20. Kay, S.M. *Fundamentals of Statistical Signal Processing*; Prentice Hall: Englewood Cliffs, NJ, USA, 1993.
21. Psiaki, M.L. Navigation using carrier Doppler shift from a LEO constellation: TRANSIT on steroids. *Navigation* **2021**, *68*, 621–641. [[CrossRef](#)]

Disclaimer/Publisher’s Note: The statements, opinions and data contained in all publications are solely those of the individual author(s) and contributor(s) and not of MDPI and/or the editor(s). MDPI and/or the editor(s) disclaim responsibility for any injury to people or property resulting from any ideas, methods, instructions or products referred to in the content.